



# Towards Routine ${}^7\text{Li}$ In Situ Solid-State NMR Studies of Electrochemical Processes in $\text{Li}|\text{LiPF}_6|\text{LFP}$ Cells

Edina Šić<sup>1</sup> · Dominion Fredericks<sup>2</sup> · Oliver Pecher<sup>3</sup> · Sebastian Wegner<sup>4</sup> · Hergen Breitzke<sup>1</sup> · Vickram Singh<sup>2</sup> · Gerd Buntkowsky<sup>1</sup> · Torsten Gutmann<sup>1</sup>

Received: 11 December 2023 / Revised: 11 December 2023 / Accepted: 12 February 2024  
© The Author(s) 2024

## Abstract

In this study, electrochemical processes in a  $\text{Li}|\text{LiPF}_6|\text{LFP}$  cell have been explored applying advanced solid-state NMR technologies. In situ solid-state NMR allows to monitor structural changes in local environments in commercially available cell components during galvanostatic cycling. In collaboration with Dragonfly Energy, ePROBE GmbH and Bruker BioSpin GmbH & Co. KG, we have demonstrated an experimental procedure for routine application of in situ solid-state NMR for battery research. This points out the high potential of this approach for use in the energy storage industry.

## 1 Introduction

Lithium-ion batteries (LIBs) constitute one of the crucial components in the development of energy storage technology [1]. Since their commercialization 30 years ago [2], continuous progress of LIB technology has been made leading to significant improvement in high-power density [3], cycling life [4] and charging conditions [5] among the alternative battery technologies. Due to these outstanding properties, LIBs find wide range applications in portable digital devices [6], electric vehicles [7] as well as stationary energy storage [8]. According to the predictions made by

---

✉ Torsten Gutmann  
gutmann@chemie.tu-darmstadt.de

Gerd Buntkowsky  
gerd.buntkowsky@tu-darmstadt.de

<sup>1</sup> Eduard Zintl Institute for Inorganic and Physical Chemistry, Technical University of Darmstadt, Peter-Grünberg-Straße 8, 64287 Darmstadt, Germany

<sup>2</sup> Dragonfly Energy, 1375 Greg St. #104, Sparks, NV 89431, USA

<sup>3</sup> ePROBE GmbH, Blumenstraße 70 Haus 3, 99092 Erfurt, Germany

<sup>4</sup> Bruker BioSpin GmbH & Co. KG, Rudolf-Plank-Straße 23, 76275 Ettlingen, Germany

McKinsey [9], the global LIB demand will rise up to 4.7 TWh over the next decade, which is in line with an increase in use of lithium energy storage systems by a factor of seven compared to the year 2022 with a demand of ca. 700 GWh. LIB technologies, however, still face challenges in their safety concerns [10], life span [11], energy density [12], costs [13] as well as environmental sustainability [14], so that further research to overcome these limitations is crucial to make them applicable for future demands.

Metallic lithium has been considered as a prospective anode material for next-generation LIBs [15]. Since lithium metal shows low electrochemical potential of  $-3.04$  V and high theoretical specific capacity of 3860 mAh/g [16], many research efforts have been made [17–21] in developing strategies to employ metallic lithium as anode to replace graphite offering a capacity of only 372 mAh/g [22]. Besides, according to recent studies [14, 23], lithium metal is eco-friendlier compared to graphite. Despite the lower environmental impact and higher energy density compared to graphite, commercialization of lithium metal anodes is challenging due to their short lifetime and safety issues caused by the high reactivity of lithium that lead to multiple side reactions in battery cells [24, 25].

Elucidation of structural changes in an electrochemical system containing lithium as anode material, while charging/discharging processes take places, is essential for understanding battery failure and improving its design. Monitoring and identification of structure moieties formed in lithium/lithium-ion electrochemical cells is still a challenging task. An electrochemical cell consisting of electrodes, electrolytes, etc., represents a complex multicomponent system, so that for its structural characterization under working condition special analytical techniques are required. In situ solid-state NMR spectroscopy (ssNMR) has been proven as a powerful tool suitable to address structural changes in local environments of electrochemical cell components during operation [26–32].

The main goal of this study is to enlighten the significance of innovative ssNMR technologies towards application for routine analysis in energy storage industry. In situ ssNMR shows great potential to become a standard approach for routine monitoring of electrochemical processes under operating conditions.

In this work, an experimental approach for routine application of in situ ssNMR for future battery studies is introduced using commercially available materials for manufacturing of lithium battery cells. As an example, the technique is demonstrated for an electrochemical cell assembled from metallic lithium as reference and counter electrode,  $\text{LiFePO}_4$  (lithium iron phosphate, LFP) as working electrode and  $\text{LiPF}_6$  (lithium hexafluorophosphate) in ethylene carbonate and dimethyl carbonate as electrolyte. Insights into cell design, cell assembly and electrochemical cycling protocol for in situ ssNMR studies of  $\text{Li}|\text{LiPF}_6|\text{LFP}$  cell are provided. Subsequently, plating and stripping of lithium metal in the cell are investigated. Hereby, it is demonstrated how in situ ssNMR allows to analyse ionic transport and to monitor microstructural changes in  $\text{Li}|\text{LiPF}_6|\text{LFP}$  as well as to investigate degradation of the electrolyte and dendrite formation at different states of charge. Such understanding of lithium deposition and degradation in electrochemical cells applying advanced ssNMR technologies significantly contributes towards the development of safe lithium metal anodes for next-generation battery technologies.

## 2 Experimental Section

### 2.1 Materials and General Procedures

Commercially available lithium iron phosphate (LFP, MTI CORP) tapes containing 93% active material and 7% PVDF/conductive carbon were baked under reduced pressure overnight (120 °C) prior to transferring into the glovebox. Lithium ribbon (Sigma-Aldrich) was freshly cut to remove any oxide layer formed on the surface. Glass fibre separators (Ahlstrom-Munksjö, thickness of ca. 0.5 mm) were baked under reduced pressure (12 h, 80 °C) and transferred into a glovebox. The electrolyte used was the following: 1 M  $\text{LiPF}_6$  (lithium hexafluorophosphate) in ethylene carbonate and dimethyl carbonate (EC:DMC 1:1 volume ratio, E-Lyte Innovations GmbH). Cell assembly and handling of air-sensitive materials were performed in an argon glovebox ( $\text{MBraun}$ ,  $\text{O}_2$ ,  $\text{H}_2\text{O} < 1$  ppm).

### 2.2 Electrochemical Cell Setup and Cycling

In Fig. 1, an electrochemical cell used for  $^7\text{Li}$  in situ solid-state NMR studies with a cylindrical geometry and an outer diameter of 15 mm is illustrated; plastic cell capsule short OD15 was provided by ePROBE [33, 34]. The cell consists of two separable cavities and a casing made from polyether ether ketone (PEEK). Inside each cell cavity, cell components such as electrodes, separator sheets, and electrolyte can be placed before assembling the cell parts by screwing a capsule/casing over the cavities. For preparing of a stable  $\text{LiLiPF}_6/\text{LFP}$  electrochemical system, 8 mg of metallic lithium and about 15.4 mg of LFP electrode (with mesh/foil) were supported on Teflon sheets and connected to the Ag/Cu wires.

The LFP electrode wetted with 50  $\mu\text{L}$  of the electrolyte solution was separated from lithium metal by placing three layers of glass fibre membranes wetted with 50  $\mu\text{L}$  of the electrolyte solution. Prior to cell assembly, the electrolyte solution was allowed to fully saturate the LFP electrode and separators for 5 min. After insertion of the separators into a cell cavity, an additional amount of ca. 100  $\mu\text{L}$  of the

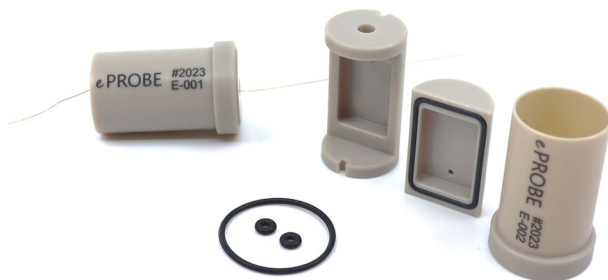


**Fig. 1** The cylindrical cell design used for assembling an  $\text{LiLiPF}_6/\text{LFP}$  electrochemical cell containing two separable cavities and a casing. Inside the cell cavities, the cell components, Teflon sheets, Ag/Cu wires, lithium metal, LFP electrode and separator sheets with  $\text{LiPF}_6$  electrolyte, were inserted. The cell cavities were attached together and fixed by the casing

LiPF<sub>6</sub> electrolyte solution was distributed over the separator/membrane sheets. Subsequently, the two cell cavity parts were aligned and compressed by a capsule/casing leading to a densely sealed electrochemical cell. The cell was soaked (1 h) after assembly before any current was applied. The as-prepared Li|LiPF<sub>6</sub>|LFP cell showed a stable voltage of about 3.4 V.

The electrochemical cycling was performed on a Bio-Logic SP-150 cycler using the EC-Lab software version 11.40. Galvanostatic cycling was carried out with potential limitation (GCPL). First, the cell voltage was increased up to 4.1 V with a rate of C/20 applying a constant current of 80  $\mu$ A. Subsequently, the cell was held at this voltage for 1 h. Afterwards, the cell voltage was decreased at the same rate down to 2.7 V where it was kept for 1 h.

### 2.3 <sup>7</sup>Li In Situ Solid-State NMR

<sup>7</sup>Li in situ ssNMR measurements were carried out on a Bruker Avance III 300 MHz NMR spectrometer at 7 T corresponding to a frequency of 116.65 MHz for <sup>7</sup>Li. Experiments were performed according to our previous works [26, 27] using a static, single-channel in situ NMR probe with automatic tuning and matching capabilities by ePROBE [29, 33, 34]. After assembling a stable Li|LiPF<sub>6</sub>|LFP cell, it was inserted to the Ag/Cu coil, oriented perpendicular with respect to the static external field B<sub>0</sub>. The probe was connected to the external electrochemical cycler (potentiostat) and automatic tuning/matching controller of the probe system [29, 33, 34]. Automatic recalibration of the carrier frequency was achieved applying low power continuous wave (cw) excitation with 0.1 W. The standing wave ratio calculated from the forwarded and reflected power was modulated to adjust capacitor positions, ensuring optimal resonance tuning. 150 MHz broadband low-pass filters were attached to the automatic tuning/matching controller in- and output ports for forwarded and reflected powers, respectively, to cut off potentially interfering frequencies during the recalibration sequence. A pseudo 2D echo sequence was used for recording of the <sup>7</sup>Li in situ ssNMR spectra employing pulses of 1.5 and 3  $\mu$ s length, respectively. These pulse lengths were adjusted on LiCl powder and correspond to 45° and 90° pulses. Note that the 45° pulse was applied to consider different quadrupolar couplings. The repetition delay was set to 1 s and 1600 scans were accumulated per each single spectrum. The <sup>7</sup>Li chemical shift was referenced with respect to the signal of a 1 M LiCl aqueous solution (0 ppm).

## 3 Results and Discussion

<sup>7</sup>Li in situ ssNMR spectra of the Li|LiPF<sub>6</sub>|LFP cell and the corresponding voltage profile between 4.1 and 2.7 V are presented in Fig. 2a. In Fig. 2b, c, an enlarged view is displayed of the <sup>7</sup>Li in situ ssNMR spectra in the range between -30 and 30 ppm, representative of ionic lithium species, and in the range between 220 and 300 ppm, representative of metallic lithium species, respectively.

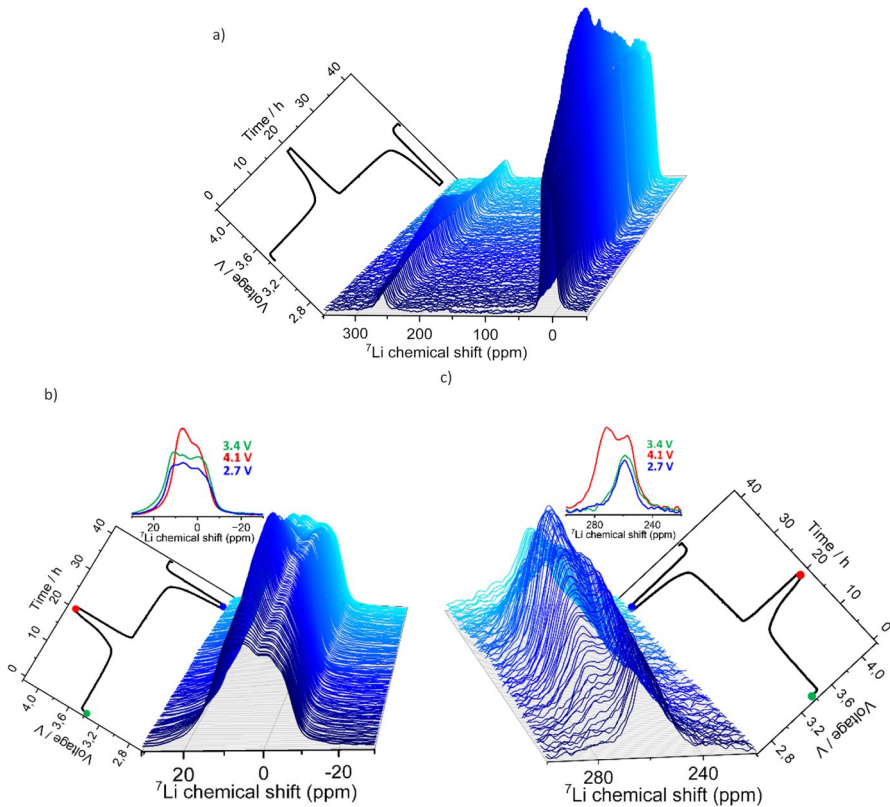


**Fig. 2** **a**  $^7\text{Li}$  in situ ssNMR spectra of the  $\text{LiLiPF}_6/\text{LFP}$  cell and corresponding voltage profile. **b** and **c** Enlarged view of the chemical shift range between  $-30$  and  $30$  ppm and of the chemical shift range between  $220$  and  $300$  ppm. Note: extracted spectra at different states of charge ( $3.4$ ,  $4.1$  and  $2.7$  V) are displayed to indicate changes observed in the  $^7\text{Li}$  in situ ssNMR spectra more distinctly

The analysis of the spectral region between  $-30$  and  $30$  ppm of the  $^7\text{Li}$  in situ ssNMR spectra obtained for the  $\text{LiLiPF}_6/\text{LFP}$  cell shows resonances at the initial state of charge at  $3.4$  V before starting the plating/stripping process. The observed resonances are attributed to lithium ions originating from the  $\text{LiPF}_6$  electrolyte [32, 35]. Hereby, it has to be noticed that the chemical shift range between  $-30$  and  $30$  ppm of the  $^7\text{Li}$  in situ ssNMR spectra is significantly broadened due to the bulk magnetic susceptibility effect of the lithium metal and the LFP electrode. Influence of the bulk magnetic susceptibility of electrodes on chemical shift and line broadening in  $^7\text{Li}$  ssNMR spectra have been explained in more details by Grey and co-workers [29, 32, 35, 36]. With increasing voltage, the signals in the region between  $-30$  and  $30$  ppm become narrower and at  $4.1$  V two clearly distinguishable resonances, a sharper one at ca.  $7$  ppm and a broader one at  $0$  ppm, become visible. These changes in the  $^7\text{Li}$  in situ ssNMR spectra are related to the mobility of lithium ions that move from the LFP electrode to the lithium metal at higher state of charge during plating.

When the voltage is decreased down to 2.7 V, the signals in the region between  $-30$  and  $30$  ppm become broader again. Overlapping resonances as visible at the initial cell state of  $3.4$  V are obtained. This observation clearly illustrates reversibility of structures formed during the plating/stripping of the  $\text{LiLiPF}_6/\text{LFP}$  cell. Note that a detailed comparison of the spectrum extracted at the initial state of charge at  $3.4$  V (Fig. 2b, green spectrum) and after the first cycle at a cutoff voltage of  $2.7$  V (Fig. 2b, blue spectrum) shows only minor changes in line shape and intensity. These differences are referred to the formation of the solid electrolyte interphase (SEI) as a result of electrolyte decomposition during the cell plating/stripping [28].

In the range between  $220$  and  $300$  ppm, all  $^7\text{Li}$  in situ ssNMR spectra of the  $\text{LiLiPF}_6/\text{LFP}$  cell (Fig. 2c) show a significant signal centred at  $257$  ppm that is present during the whole charging/discharging process. This signal is attributed to lithium metal applied as counter electrode [35]. The rises in intensity of this signal with higher voltage clearly demonstrates that the detectable lithium metal amount changes. Next to this signal, a shoulder peak at  $271$  ppm is visible which evolves significant intensity growth during cell plating. The changes in intensity and broadening of this shoulder peak are strongly pronounced, so that the shoulder signal at  $271$  ppm and the lithium metal signal at  $257$  ppm cannot be distinguished at  $4.1$  V. This finding suggests deposition of lithium metal on the lithium metal electrode and its further accumulation with cycling [28, 32]. The shoulder peak of plated lithium metal drops down in intensity when the voltage is decreased and vanishes completely at the cutoff voltage of  $2.7$  V. From these observations, it can be assumed that the formed lithium metallic structures were stripped away from the lithium metal electrode.

## 4 Conclusion

An electrochemical  $\text{LiLiPF}_6/\text{LFP}$  cell was successfully prepared showing an initial voltage of  $3.4$  V. The cell was cycled in the voltage window between  $4.1$  and  $2.7$  V to monitor structural changes applying  $^7\text{Li}$  in situ ssNMR during lithium plating/stripping. All  $^7\text{Li}$  in situ ssNMR spectra show changes depending on the state of the cell charge. In the spectral range between  $-30$  and  $30$  ppm, a significant narrowing of line width with increasing voltage is visible which is reversible when decreasing the voltage and thus indicates mobility of lithium ions. At the same time, a signal at  $271$  ppm close to the lithium metal peak at  $257$  ppm appears, suggesting that active lithium metal had been plated on the lithium metal electrode.

In summary, it has been shown that the commercially available in situ battery ssNMR setup is suitable to investigate new electrochemical cells using commercially available cell compounds. Successful application of in situ ssNMR technology is demonstrated to investigate electrochemical processes in a multicomponent system during cell operation. Based on our studies performed on an  $\text{LiLiPF}_6/\text{LFP}$  cell, we proposed that our in situ ssNMR approach is suitable for routine use in industrial energy storage applications.

**Author Contributions** E.S. did the in-situ NMR experiments and their analysis, and wrote the manuscript draft. D.F. supported the cell assembly of the LiLiPF<sub>6</sub>LFP. O.P. organized the exchange between the partners, and provided support for the in-situ probe setup. S.W. supported the performance of NMR experiments, and corrected the manuscript. H.B. provided technical support of the experiments as head of the NMR lab in Darmstadt. V.S. supported the cell assembly of the LiLiPF<sub>6</sub>LFP, and provided the electrode materials. G.B. co-supervised the project, and corrected the manuscript. T.G. supervised the project, conceived and processed the manuscript, and supported the experiments and data analysis.

**Funding** Open Access funding enabled and organized by Projekt DEAL.

**Availability of Data and Materials** Data supporting the findings of this study are available upon request.

## Declarations

**Conflict of Interest** The authors declare no conflict of interest.

**Ethical Approval** This research does not contain any studies involving animal or human participants, nor did it take place in any private or protected areas.

**Open Access** This article is licensed under a Creative Commons Attribution 4.0 International License, which permits use, sharing, adaptation, distribution and reproduction in any medium or format, as long as you give appropriate credit to the original author(s) and the source, provide a link to the Creative Commons licence, and indicate if changes were made. The images or other third party material in this article are included in the article's Creative Commons licence, unless indicated otherwise in a credit line to the material. If material is not included in the article's Creative Commons licence and your intended use is not permitted by statutory regulation or exceeds the permitted use, you will need to obtain permission directly from the copyright holder. To view a copy of this licence, visit <http://creativecommons.org/licenses/by/4.0/>.

## References

1. M.M. Hamed, A. El-Tayeb, I. Moukhtar, A.Z. El Dein, E.H. Abdelhameed, A review on recent key technologies of lithium-ion battery thermal management: external cooling systems. *Results Eng.* **16**, 100703 (2022). <https://doi.org/10.1016/j.rineng.2022.100703>
2. Y. Nishi, Lithium ion secondary batteries; past 10 years and the future. *J. Power Sour.* **100**, 101–106 (2001). [https://doi.org/10.1016/S0378-7753\(01\)00887-4](https://doi.org/10.1016/S0378-7753(01)00887-4)
3. B. Rowden, N. Garcia-Araez, Estimating lithium-ion battery behavior from half-cell data. *Energy Rep.* **7**, 97–103 (2021). <https://doi.org/10.1016/j.egy.2021.02.048>
4. A. Yoshino, The birth of the lithium-ion battery. *Angew. Chem. Int. Ed.* **51**, 5798–5800 (2012). <https://doi.org/10.1002/anie.201105006>
5. S. Li, K. Wang, G. Zhang, S. Li, Y. Xu, X. Zhang, X. Zhang, S. Zheng, X. Sun, Y. Ma, Fast charging anode materials for lithium-ion batteries: current status and perspectives. *Adv. Func. Mater.* **32**, 2200796 (2022). <https://doi.org/10.1002/adfm.202200796>
6. A. Manthiram, Materials challenges and opportunities of lithium ion batteries. *J. Phys. Chem. Lett.* **2**, 176–184 (2011). <https://doi.org/10.1021/jz1015422>
7. X. Zeng, M. Li, D. Abd El-Hady, W. Alshitari, A.S. Al-Bogami, J. Lu, K. Amine, Commercialization of lithium battery technologies for electric vehicles. *Adv. Energy Mater.* (2019). <https://doi.org/10.1002/aenm.201900161>
8. T. Günther, N. Billot, J. Schuster, J. Schnell, F.B. Spingler, H.A. Gasteiger, The manufacturing of electrodes: key process for the future success of lithium-ion batteries. *Adv. Mater. Res.* **1140**, 304–311 (2016). <https://doi.org/10.4028/www.scientific.net/AMR.1140.304>

9. J. Fleischmann, M. Hanicke, E. Horetsky, D. Ibrahim, S. Jautelat, M. Linder, P. Schaufuss, L. Torscht, A. van de Rijt, Battery 2030: Resilient, Sustainable and circular, McKinsey & Global Battery Alliance (2023).
10. Y. Chen, Y. Kang, Y. Zhao, L. Wang, J. Liu, Y. Li, Z. Liang, X. He, X. Li, N. Tavajohi, B. Li, A review of lithium-ion battery safety concerns: the issues, strategies, and testing standards. *J. Energy Chem.* **59**, 83–99 (2021). <https://doi.org/10.1016/j.jechem.2020.10.017>
11. M. Shahjalal, T. Shams, M.E. Islam, W. Alam, M. Modak, S.B. Hossain, V. Ramadesigan, M.R. Ahmed, Hafiz Ahmed, A. Iqbal, A review of thermal management for Li-ion batteries: prospects, challenges, and issues. *J. Energy Storage* (2021). <https://doi.org/10.1016/j.est.2021.102518>
12. L.S. Zhang, X.L. Gao, X.H. Liu, Z.J. Zhang, R. Cao, H.C. Cheng, M.Y. Wang, X.Y. Yan, S.C. Yang, CHAIN: unlocking informatics-aided design of Li metal anode from materials to applications. *Rare Met.* **41**, 1477–1489 (2022). <https://doi.org/10.1007/s12598-021-01925-8>
13. T. Chen, Y. Jin, H. Lv, A. Yang, M. Liu, B. Chen, Y. Xie, Q. Chen, Applications of lithium-ion batteries in grid-scale energy storage systems. *Trans. Tianjin Univ.* **26**, 208–217 (2020). <https://doi.org/10.1007/s12209-020-00236-w>
14. H. Berg, M. Zackrisson, Perspectives on environmental and cost assessment of lithium metal negative electrodes in electric vehicle traction batteries. *J. Power Sour.* **415**, 83–90 (2019). <https://doi.org/10.1016/j.jpowsour.2019.01.047>
15. J.F. Ding, R. Xu, N. Yao, X. Chen, Y. Xiao, Y.X. Yao, C. Yan, J. Xie, J.Q. Huang, Non-solvating and low-dielectricity cosolvent for anion-derived solid electrolyte interphases in lithium metal batteries. *Angew. Chem. Int. Ed.* **60**, 11442–11447 (2021)
16. Y. Zhang, W. Luo, C. Wang, Y. Li, C. Chen, J. Song, J. Dai, E.M. Hitz, S. Xu, C. Yang, Y. Wang, Hu. Liangbing, High-capacity, low-tortuosity, and channel-guided lithium metal anode. *Proc. Natl. Acad. Sci.* **114**, 3584–3589 (2017). <https://doi.org/10.1073/pnas.1618871114>
17. S.H. Lee, J.Y. Hwang, J. Ming, Z. Cao, H.A. Nguyen, H.G. Jung, J. Kim, Y.K. Sun, Toward the sustainable lithium metal batteries with a new electrolyte solvation chemistry. *Adv. Energy Mater.* **10**, 2000567 (2020). <https://doi.org/10.1002/aenm.202000567>
18. V. Marangon, L. Minnetti, M. Adami, A. Barlini, J. Hassoun, Lithium-metal batteries using sustainable electrolyte media and various cathode chemistries. *Energy Fuels Am. Chem. Soc. J.* **35**, 10284–10292 (2021). <https://doi.org/10.1021/acs.energyfuels.1c00927>
19. L. Yu, N.L. Canfield, S. Chen, H. Lee, X. Ren, M.H. Engelhard, Q. Li, J. Liu, W. Xu, J.G. Zhang, Enhanced stability of lithium metal anode by using a 3D porous nickel substrate. *ChemElectroChem* **5**, 761–769 (2018). <https://doi.org/10.1002/celec.201701250>
20. S. Li, J. Huang, Y. Cui, S. Liu, Z. Chen, W. Huang, C. Li, R. Liu, R. Fu, D. Wu, A robust all-organic protective layer towards ultrahigh-rate and large-capacity Li metal anodes. *Nat. Nanotechnol.* **17**, 613–621 (2022). <https://doi.org/10.1038/s41565-022-01107-2>
21. Q. Zhao, X. Chen, W. Hou, B. Ye, Y. Zhang, X. Xia, J. Wang, A facile, scalable, high stability lithium metal anode. *SusMat* (2022). <https://doi.org/10.1002/sus2.43>
22. X. Zhao, V.-P. Lehto, Challenges and prospects of nanosized silicon anodes in lithium-ion batteries. *Nanotechnology* **32**, 42002 (2021). <https://doi.org/10.1088/1361-6528/abb850>
23. Z. Wu, D. Kong, Comparative life cycle assessment of lithium-ion batteries with lithium metal, silicon nanowire, and graphite anodes. *Clean Technol. Environ. Policy* **20**, 1233–1244 (2018). <https://doi.org/10.1007/s10098-018-1548-9>
24. M. Winter, J.O. Besenhard, M.E. Spahr, P. Novak, Insertion electrode materials for rechargeable lithium batteries. *Adv. Mater.* **10**, 725–763 (1998). [https://doi.org/10.1002/\(SICI\)1521-4095\(199807\)10:10%3c725::AID-ADMA725%3e3.0.CO;2-Z](https://doi.org/10.1002/(SICI)1521-4095(199807)10:10%3c725::AID-ADMA725%3e3.0.CO;2-Z)
25. K. Kanamura, Secondary batteries—lithium rechargeable systems | negative electrodes: lithium metal. *Encycl. Electrochem. Power Sour.* (2009). <https://doi.org/10.1016/B978-044452745-5.00191-X>
26. E. Šić, K. Schutjajew, U. Haagen, H. Breitzke, M. Oschatz, G. Buntkowsky, T. Gutmann, Electrochemical sodium storage in hard carbon powder electrodes implemented in an improved cell assembly: insights from in-situ and ex-situ solid-state NMR. *ChemSusChem* (2023). <https://doi.org/10.1002/cssc.202301300>
27. E. Šić, M. Melzi d’Eril, K. Schutjajew, M.J. Graczyk-Zajac, H. Breitzke, R. Riedel, M. Oschatz, T. Gutmann, G. Buntkowsky, SiCN ceramics as electrode materials for sodium/sodium ion cells—insights from <sup>23</sup>Na in-situ solid-state NMR. *Batteries Supercaps* (2022). <https://doi.org/10.1002/batt.202200066>



28. Y.-C. Hsieh, M. Leißing, S. Nowak, B.-J. Hwang, M. Winter, G. Brunklaus, Quantification of dead lithium via in situ nuclear magnetic resonance spectroscopy. *Cell Rep. Phys. Sci.* **1**, 100139 (2020). <https://doi.org/10.1016/j.xcrp.2020.100139>
29. O. Pecher, P.M. Bayley, H. Liu, Z. Liu, N.M. Trease, C.P. Grey, Automatic tuning matching cyclers (ATMC) in situ NMR spectroscopy as a novel approach for real-time investigations of Li- and Na-ion batteries. *J. Magn. Reson.* **265**, 200–209 (2016). <https://doi.org/10.1016/j.jmr.2016.02.008>
30. K. Gotoh, T. Yamakami, I. Nishimura, H. Kometani, H. Ando, K. Hashi, T. Shimizu, H. Ishida, Mechanisms for overcharging of carbon electrodes in lithium-ion/sodium-ion batteries analysed by operando solid-state NMR. *J. Mater. Chem. A* **8**, 14472–14481 (2020). <https://doi.org/10.1039/D0TA04005C>
31. F. Poli, J.S. Kshetrimayum, L. Monconduit, M. Letellier, New cell design for in-situ NMR studies of lithium-ion batteries. *Electrochem. Commun.* **13**, 1293–1295 (2021). <https://doi.org/10.1016/j.elecom.2011.07.019>
32. A.B. Gunnarsdóttir, C.V. Amanchukwu, S. Menkin, C.P. Grey, Noninvasive in situ NMR study of “dead lithium” formation and lithium corrosion in full-cell lithium metal batteries. *J. Am. Chem. Soc.* **142**, 20814–20827 (2020). <https://doi.org/10.1021/jacs.0c10258>
33. O. Pecher, S. Wegner, Battery research probes for Li-ion technologies (and beyond), Application Note ePROBE GmbH and Bruker BioSpin GmbH (2023).
34. O. Pecher, J. Carretero-González, K.J. Griffith, C.P. Grey, Materials’ methods: NMR in battery research. *Chem. Mater.* **29**, 213–242 (2017). <https://doi.org/10.1021/acs.chemmater.6b03183>
35. N.M. Trease, L. Zhou, H.J. Chang, B.Y. Zhu, C.P. Grey, In situ NMR of lithium ion batteries: bulk susceptibility effects and practical considerations. *Solid State Nucl. Magn. Reson.* **42**, 62–70 (2012). <https://doi.org/10.1016/j.ssnmr.2012.01.004>
36. L. Zhou, M. Leskes, A.J. Ilott, N.M. Trease, C.P. Grey, Paramagnetic electrodes and bulk magnetic susceptibility effects in the in situ NMR studies of batteries: application to  $\text{Li}_1.08\text{Mn}_{1.92}\text{O}_4$  spinels. *J. Magn. Resonance* (2013). <https://doi.org/10.1016/j.jmr.2013.05.011>

**Publisher's Note** Springer Nature remains neutral with regard to jurisdictional claims in published maps and institutional affiliations.